COLLOIDS AND SURFACES A

Colloids and Surfaces A: Physicochem. Eng. Aspects 255 (2005) 165–180

Effect of NaCl and temperature on the water solubilization behavior of AOT/nonionics mixed reverse micellar systems stabilized in IPM oil

Rajib K. Mitra, Bidyut K. Paul*

Geological Studies Unit, Indian Statistical Institute, 203 B.T. Road, Kolkata 700108, India

Received 19 June 2004; accepted 21 December 2004
Available online 26 January 2005

Abstract

Solubilization of water in mixed reverse micellar systems formed with anionic surfactant (AOT) and nonionic surfactants (Brij-30, Brij-35, Brij-52, Brij-56, Brij-58, Brij-76, Tween-20, Tween-40, Span-20, Span-40, Span-60, Span-80) in isopropyl myristate (IPM) oils has been studied. The enhancement in water solubilization (i.e. synergism) has been evidenced by the addition of nonionic surfactants to AOT/IPM system. The maximum water solubilization capacity ($\omega_{0,max}$) and the mole fraction of nonionic surfactant at which maximization occurs ($X_{nonionic,max}$) in these mixed reverse micellar systems has been found to depend on surfactant component (size and nature of polar group and hydrocarbon moiety of the surfactant). The addition of electrolyte (NaCl) in these systems has been found to enhance the solubilization capacity (ω_{max}) depending upon the content and their EO chains and type of polar head group of nonionic surfactant used. The maximum solubilization of electrolyte, ω_{max} was obtained at an optimal concentration of it ($[NaCl]_{max}$), which depends on the content and their EO chains and type of polar heads of the nonionic surfactants. The temperature induced solubilization of water (in absence and presence of additives) for AOT blended with nonionic surfactants (Brijs, Tweens, Spans) at different compositions has been investigated. The stability of these systems with respect to temperature has been found to be dependent on the content and nature of the polar head group as well as the hydrophobic moiety of the nonionics. The energetic parameters ($\Delta\bar{G}^\circ$, $\Delta\bar{H}^\circ$ and $\Delta\bar{S}^\circ$) of the desolubilization process of water in the mixed systems have been estimated from the solubilization capacity–temperature profile. An attempt has been made to shed more insight into the process of solubilization–desolubilization of water (or aqueous NaCl) in mixed reverse micelles stabilized in IPM oil on the basis of the model proposed by Shah et al. [M.J. Hou, D.O. Shah, Langmuir 3 (1987) 1086; R. Leung, D.O. Shah, J. Colloid Interf. Sci. 120 (1987) 320, 330] and thermodynamic approach.

Keywords: Mixed reverse micelles; Solubilization; IPM; AOT; Brijs; Energetic parameters

1. Introduction

The term "solubilization" was first defined by McBain and Hutchinson [1]. According to them, solubilization is the increase in the solubility of an insoluble substance in a given medium. Recently, Nagarajan [2] defined the phenomenon of solubilization as an increase in the solubility of solvophobic substances in a solvent medium caused by the presence of amphiphilic aggregates. Owing to diphilic nature, surfactants are well known to self-assemble in solutions and can solubilize water in otherwise immiscible organic solvents. Surfactant molecules form monolayer film between water and oil phases in order to stabilize the formation and orient with their polar head groups directed towards the centre of the micelle and the hydrocarbon tails protruding into the surrounding medium. Such systems are referred to as a reverse micelles, which are isotropic and homogeneous on a macroscopic scale while heterogeneous on a microscopic scale and can be viewed as nanometer scale droplets of water suspended in an organic continuum (forming a so-called water pool) rendered thermodynamically stable by the surfactant. These reverse micellar aggregates exhibit the remarkable ability to solubilize large amount of water, resulting in the formation of water-in-oil (w/o) microemulsions. The properties of water molecules localized in the interior of the

reverse micelles are physicochemically different from those of bulk water, the difference becoming progressively smaller as the water content in the micellar system increases [3,4]. During the last 50 years there have been many investigations regarding the factors leading to reverse micelle formation, and basic properties of reverse micellar solutions with special references to their structural aspects, state of water, properties of the interface, thermodynamics of their formation process, photochemistry, etc. [4–9]. Reverse micellar systems have now-a-days attracted the attention of research workers from various fields of science and technology due to their potential uses in industry and technology [10–17]. The solubilized water in reverse micellar system shows close similarity to biological membrane and proteins and hence is treated as model for many biologically important systems [18–24]. Solubilization of an insoluble molecule in a surfactant solution is primarily governed by fundamental properties linked to thermodynamics and structure [25]. The solubilization capacity of water in reverse micellar system depends upon factors, such as the rigidity of the interfacial film, which in turn depends upon the area and nature of the polar head group and the hydrocarbon chain of the surfactant, composition, temperature, presence of electrolytes, type of the solvent, valance of counterion, etc. [10,26,27].

Studies on the extent of water solubilization in reverse micelle was initiated by Kon-No and Kitahara [26,28,29]. They studied the secondary solubilization (solubilization of a water-soluble substance into the water that is solubilized in the reverse micelle) of various electrolytes of different charge types in different single surfactant systems (dodecyl ammonium carboxylate, polyoxyethylene nonylphenyl ether, AOT) in organic solvents at different temperatures. They concluded that the maximum amount of solubilized water was higher in the presence of electrolyte, and a specific temperature of maximum solubilization was observed for each type of electrolyte. These results were explained on the basis of Lewis acid–base theory and Derjaguin–Landau–Verway–Overbeek theory. They [30] also investigated on the solubilization behavior of AOT reverse micellar systems in paraffin, napthenic, and aromatic solvents and the effect of the size and alkyl side chain of the solvent on the solubilization behavior.

Shah and coworkers [31–34] carried out fundamental work in this field to underline the factors governing solubilization in reverse micellar systems. The effects of the molecular structure of interface and the continuous phase on the solubilization capacity of water in w/o microemulsions stabilized by AOT in hydrocarbon oils have been reported from both theoretical considerations and experimental observations. They explained the maximization in solubilization capacity as a competition between two opposing factors, arising out of the rigidity of the interface (which depends upon the spontaneous radius of curvature, R_0 and elasticity constant k) and the attractive interaction among the droplets (governed by the critical radius of curvature R_c). Factors like molecular volume, chain length and chemical structure of oil, salinity, chain length of cosurfactants, and area of polar head group of surfactants are observed to affect k and R_c and thereby govern the solubilization phenomenon. They also reported on the effect of additives (nonionic surfactants, electrolytes, alcohols, etc.) on the solubilization behavior of such systems. Bansal et al. [35] studied the solubilization capacity of w/o microemulsions formed with fatty acids soaps and alcohols as a function of alkyl chain of oil, soap and alcohol, and found that the maximum in solubilization was observed when chain length compatibility was reached. Zana and coworkers [36] carried out systematic work to underline the solubilization phenomena involving cationic surfactants in various aromatic solvents. They interpreted their results in the light of the model developed by Shah and coworkers [31–33].

Kawai et al. [37,38] reported on the limiting amounts of water solubilized by anionic surfactant (AOT) in different hydrocarbon oils (cyclohexane, heptene, *iso*-octane, dodecane and toluene) and cationic surfactant (butyldodecyl dimethyl ammonium bromide, BDDAB) in chlorobenzene. They found that the magnitude of solubilization capacity of water for AOT-based systems in different oils follows the order: heptane > cyclohexane > *iso*-octane > dodecane > toluene. They obtained different states of water as a function of ω_0 (=[H_2O]/[surfactant]) for both these systems using ^{1}NMR, fluorescence and near infrared spectroscopic techniques. Very recently, they [39] measured the limiting amounts of solubilized aqueous NaCl, $NaNO_3$, $MgCl_2$ and $AlCl_3$ in AOT/*iso*-octane solution as a function of the ionic strength of the electrolytes. In each system, an optimal ionic strength was reported and the results were interpreted in terms of salting-in and salting-out phenomena as well as from the counteracting effects of attractive intermicellar interaction and interfacial bending stress.

An important aspect of studies involving reverse micellar systems is its ability to solubilize a substantial amount of water as the dispersed phase into the continuous oil phase. Single surfactant does not necessarily produce such maximization. It is well known that mixtures of surfactants often give rise to enhanced performance over the individual components for a wide variety of applications [40,41] and thus it is expected that enhanced solubilization of water in reverse micelles or water-in-oil (w/o) microemulsion can also be achieved with surfactant mixtures.

Reports on the solubilization of water and properties of solubilized water in AOT, DDAB [42,43] and Igepal CO 520 [44] based reverse micellar systems in hydrocarbon oils are available in literature, but such studies with mixed surfactants (anionic–nonionic, cationic–non-ionic, nonionic–nonionic) are scarce. Synergism in water solubilization has been reported by Shah and coworkers [45] for anionic (AOT)–nonionic (Span 20) blends of different proportions in hexadecane oil. Later they extended their study [46] to examine the solubilization behavior of water in mixed reverse micellar systems stabilized by nonionic–nonionic surfactant blends in cyclohexane oil using different nonylphenyl ethoxylates (C_9PhE_n, Igepal series) with different HLB

values. They found increase in solubilization capacity (synergism) on mixing surfactants with different HLB values and suggested two different synergism mechanisms. Ludensten et al. [47] reported an enhancement in water solubilization capacity in mixed surfactant water-in-oil (w/o) microemulsion systems consisting of anionic surfactant (AOT) and nonionic (alkyl phenyl ethoxylates with different number of EO groups) in aromatic oils (benzene, toluene, *p*-xylene and mesitylene). They concluded that hydrophobicity of oils played a role on water solubility in these systems. Seedher and Manik [48] investigated the solubilization capacity of blends of cationic (CTAB, CPB) or anionic surfactant (AOT) with nonionic surfactant (Brij-30, Triton-X-100) mixtures in hydrocarbon oils (cyclohexane, hexane, octane, benzene) and showed that the solubilization of water increased significantly with the incorporation of nonionic surfactant.

Liu et al. [49] reported on the solubilization of water and aqueous NaCl solution in mixed reverse micellar systems formed with anionic surfactant (AOT) and nonionic surfactants (Brij-30, 52, 56 and 58) in cyclohexane, *n*-hexane, *n*-heptane, *n*-octane and *iso*-octane oils. They found that solubilization capacity of water reached a maximum value ($\omega_{0,\max}$) in presence of a certain concentration of NaCl ($C_{\max}$), which in turn has been found to depend upon the content and EO chain length of the nonionic surfactants and molar volume of the oils. Li et al. [50] investigated the influence of two typical additives, long chain organic molecule, bis (2-ethylhexyl) phosphoric acid (HDEHP) and inorganic electrolyte (NaCl) on the water solubilization capacity of AOT and NaDEHP in *n*-heptane solutions. The effects of the variable (additives, water content and temperature) on the water solubilization capacity and structure of oil–water interface have also been examined by measuring the electrical conductivity of these systems. Eastoe and coworkers [51] have studied the solubilization and structural aspects of mixed reverse micellar systems solubilized by cationic surfactant DDAB and its mixture with cationic DTAB, nonionic $C_{12}E_5$ and anionic SDS in heptane oil. The cationic–cationic blend increased the solubilization capacity but is decreased in the case of cationic–anionic mixture.

In this paper, we report the water solubilization behavior of mixed surfactant reverse micellar systems stabilized by AOT/nonionic (Brijs, Tweens, Spans) blends in isopropyl myristate (IPM) oil. IPM oil has widely been used in biologically relevant microemulsion systems [52–54], but has never been reported as a media for reverse micellar systems. This oil is different from hydrocarbon oils in respect of its structure and polarity. We previously reported that conductance behavior of AOT/nonionics/IPM/water systems are different from those stabilized in hydrocarbon systems [55a]. In continuation of this study, we herein investigated the solubilization behavior of AOT/nonionics/IPM/water systems and also report the effect of electrolyte (NaCl) and other additives (cholesterol and urea) on the solubilization behavior as well as the stability of these formulations with respect to temperature. The selection of the additives was not arbitrary, as justification for using these kind of additives has been reported in our earlier work [55b]. Energetic parameters (free energy, enthalpy and entropy) have also been estimated from the temperature induced solubilization behavior of such systems. An attempt has been made to explain solubilization phenomenon in mixed reverse micelles on the basis of the model proposed by Shah and coworkers [31–33] together with thermodynamic consideration.

2. Materials and methods

The following surfactants were used without further purification: sodium bis (2-ethylhexyl) sulfosuccinate (AOT, 99%), polyoxyethylene(20) sorbitanmonolaurate (Tween-20), polyoxyethylene(20) sorbitanmonopalmitate (Tween-40) were purchased from Sigma, USA. Polyoxyethylene(4) lauryl ether (Brij-30), polyoxyethylene(10) lauryl ether (Brij-35), polyoxyethylene(2) cetyl ether (Brij-52), polyoxyethylene(10) cetyl ether (Brij-56), polyoxyethylene(20) cetyl ether (Brij-58), polyoxyethylene(10) stearyl ether (Brij-76), sorbitan monolaurate (Span-20), sorbitan monopalmitate (Span-40), sorbitan monostearate (Span-60), sorbitan monooleate (Span-80) are products of Fluka (Switzerland). Chemical structures of some of the surfactants are presented in Scheme 1. NaCl and urea are products of SRL, India, and are of AR and extrapure grade. Isopropyl myristate (IPM) is a product of Fluka (Switzerland) and its density and refractive index agreed well with the literature. Cholesterol was a product of Sigma, USA. Sudan IV and Eosin Blue are AR grade products of SRL, India.

Double distilled water with conductance less than $3\,\mu S\,cm^{-1}$ was used. Stock solutions of all the surfactants as mentioned above were made in IPM, and mixed anionic (AOT) in different proportions with nonionic surfactants to vary X_{nonionic}, where X denotes the mole fraction of nonionic surfactant in total surfactant ($X_{\text{nonionic}} = [\text{nonionic}]/([\text{nonionic}] + [\text{ionic}])$). The surfactant solution was fixed at a concentration of 0.1 mol dm^{-3}. These solutions were taken in sealed test tubes, equilibrated in thermostatic water bath at specified temperatures and titrated with water [or aqueous NaCl of different concentrations] using microsyringe of varying capacity with constant stirring in a vortex shaker. The onset of permanent turbidity at each composition of surfactant mixture in oil denotes maximum solubilization of water or aqueous NaCl at the end point of titration. All the experiments were repeated 2–3 times and mean results were taken. In order to check the behavior of the phase separation at the saturation of solubilization (i.e. at equilibrium), we used two dyes: Eosin Blue (EB), which is selectively soluble in water and Sudan IV, which is selectively soluble in oils [33,49]. These systems were allowed at least 1 h time at specified temperature in order to ensure complete phase separation. The different phases as well as Winsor types have been identified in accordance with the different colours developed due to the solubilization of these two dyes (of different characteristics)

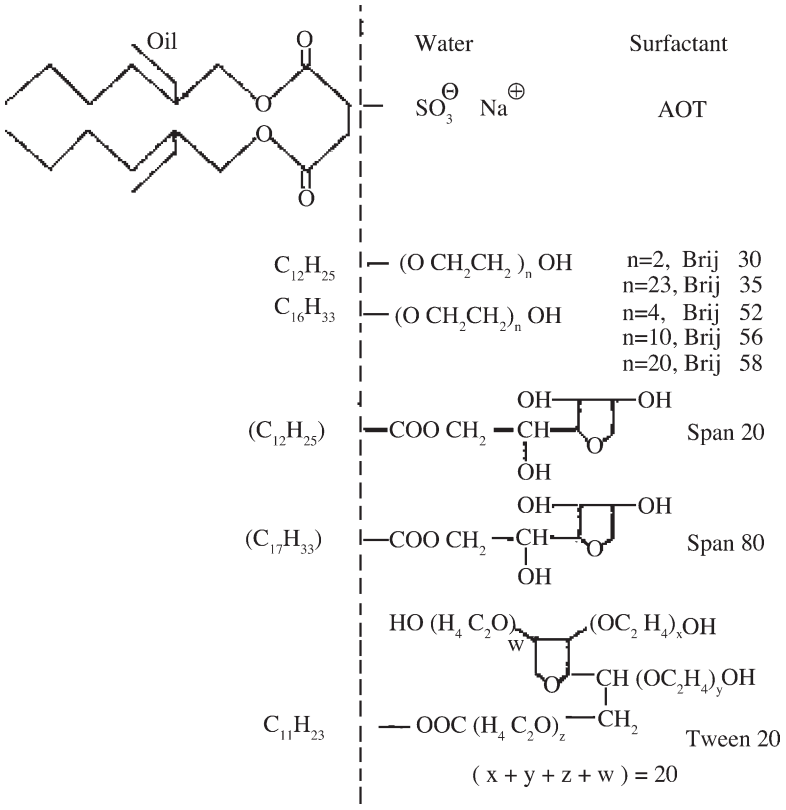

Scheme 1.

in these mixed systems. The results of these experiments have been dealt in the subsequent section. To study the effect of temperature in these systems, solutions with fixed composition (ω) were prepared in sealed test tubes and kept in a thermostatic water bath. Temperature of the bath was increased at an interval of 1 °C and at each temperature, the test tubes were shaken vigorously and then kept in the thermostat to attain equilibrium. After attainment of equilibrium, phase characteristics were noted at each temperature. The temperature at which the formulation gets turbid corresponds to the optimum solubilization temperature (T_U).

3. Results and discussion

3.1. Water solubilization capacity of AOT/nonionic/IPM systems

AOT reverse micelles in IPM with total surfactant concentration of 0.1 mol dm^{-3} can solubilize water upto ω_0([water]/[surfactant]) ~ 22. When AOT was blended with nonionic surfactants (Brijs), the solubilization capacity increased up to a maximum value ($\omega_{0,max}$) at a certain mole fraction of the nonionic surfactant, $X_{nonionic,max}$ beyond which the solubilization capacity decreased with increasing $X_{nonionic}$. The result of solubilization behavior of these mixed systems has been presented in Fig. 1 and Table 1. It can be observed from Fig. 1 and Table 1 that solubilization maximum was obtained at a low $X_{nonionic,max}$ value (0.05) for AOT/Brij-35 and AOT/Brij-58 blends, whereas it has higher values for AOT/Brij-30 and AOT/Brij-52 blends (0.2 and 0.3, respectively). For the AOT/Brij-56 and AOT/Brij-76 blends, maximization occurred at X_{Brij} = 0.1 and 0.05, respectively. It can be noted that Brij-35 and Brij-58 have 23 and 20 POE chains in their polar head groups, whereas Brij-30, Brij-52 and Brij-56 have 4, 2 and 10 POE chains, respectively, in their head groups. Thus it can be inferred that solubilization max-

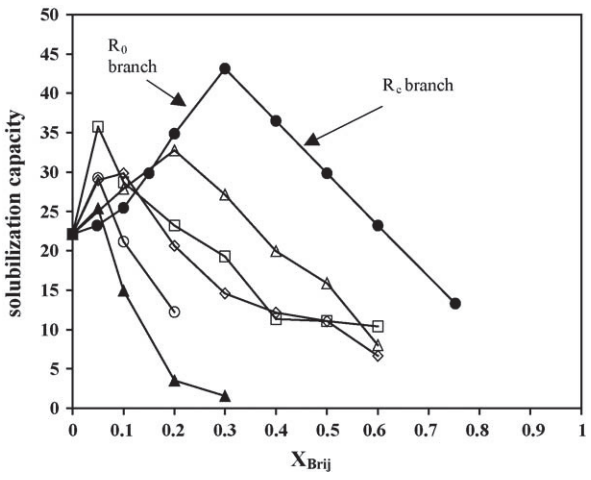

Fig. 1. Solubilization capacity of water in AOT/nonionic/IPM reverse micellar system at 303 K with total surfactant concentration 0.1 mol dm^{-3}: (□) AOT/Brij-76; (△) AOT/Brij-30; (◇) AOT/Brij-56; (●) AOT/Brij-52; (▲) AOT/Brij-35; (○) AOT/Brij-58.

Table 1
Solubilization of water ($\omega_{0,max}$) in mixed reverse micellar system AOT/nonionics/IPM/water at 303 K[a]

Nonionic surfactant	$\omega_{0,max}$[b]	$X_{nonionic,max}$[b]
Brij-30	32.8	0.2
Brij-35	25.4	0.05
Brji-52	43.2	0.3
Brji-56	30.0	0.1
Brji-58	29.0	0.05
Brji-76	35.8	0.05
Tween-20	27.3	0.05
Tween-40	30.0	0.05
Span-20	42.5	0.4
Span-40	50.0	0.3
Span-60	52.5	0.3
Span-80	55.0	0.3

[a] ω_0, represents [water]/[AOT] in IPM at $[S_T] = 0.1$ mol dm^{-3} and is equal to 22.1 at 303 K.
[b] $\omega_{0,max}$ and $X_{nonionic,max}$ represent the maximum solubilization of water at a particular mole fraction of nonionic surfactant.

imum occurred at a low $X_{nonionic,max}$ for nonionic surfactants with larger polar head groups than those having smaller head groups. The highest $\omega_{0,max}$ was obtained for AOT/Brij-52 blend, whereas that for AOT/Brij-35 was the smallest.

Solubilization of water in reverse micellar system depends upon many factors, for example, type of surfactant (and cosurfactant/a second surfactant), oil, temperature, and additives, etc. [49]. But the main driving force of such solubilization is the spontaneous curvature and the elasticity (or rigidity) of the interfacial film formed by the surfactant system [31]. If the interfacial curvature and the bending elasticity are fixed, solubilization can be maximized by minimizing the interfacial bending stress of the rigid interface and the attractive interdroplet interaction [42]. The critical packing parameter (CPP, given by $P = v/al$ where v and l are the volume and the length of hydrophobic chain, respectively, and a the area of polar head group of the surfactant) of the surfactant plays an important role in water solubilization.

The solubilization phenomenon in reverse micellar systems stabilized by AOT/hydrocarbons can be explained on the basis of the model developed by Shah and coworkers [31–33]. According to them, the growth of microemulsion droplets during the solubilization process and consequently the phase separation in such systems is limited by two opposing factors, namely the radius of spontaneous curvature (R_0) as the result of curvature effect, and by the critical radius of droplets (R_c), due to the result of attractive interaction among the droplets. The curvature effect is related to the cohesive force between the hydrocarbon chains at the interface as well as to the rigidity of the interface. For such systems, the solubilization capacity can be increased by any modification of the molecular structure of either the interface or continuous phase so that R_0 is increased. This model predicts that at a given surfactant concentration, the maximum solubilization capacity of the system can be obtained by adjusting the interfacial curvature and elasticity to optimum values at which the bending stress and the attractive forces of the interface are both minimized. Hence, one can increase the solubilization of a microemulsion with a rigid interface by increasing its natural radius and fluidity of the interface. On the other hand, the solubilization of a microemulsion of a fluid interface can be increased by increasing the interfacial rigidity and decreasing the natural radius.

In the present study, we performed dye solubilization experiment [33,49] to estimate the phase separation phenomenon in single AOT/IPM/water as well as mixed AOT/nonionics/IPM/water with $X_{nonionic} < X_{nonionic,max}$ and $X_{nonionic} \geq X_{nonionic,max}$. The results have been depicted through solubilization capacity versus X_{Brij} profile in Fig. 1. For the single surfactant system AOT/IPM/water and mixed system AOT/nonionic/IPM/water with $X_{nonionic} < X_{nonionic,max}$, it has been found that after complete phase separation (upon addition of excess water), when an oil soluble dye Sudan IV was added into it, the upper phase became intense red, whereas the lower phase remained colourless. On the other hand, upon addition of a water soluble dye, Eosin Blue, the lower phase became intensely violet and the upper phase faintly violet. This study points out to the fact that the lower phase is a pure aqueous phase in equilibrium with an upper microemulsion phase (Winsor II type). Thus the phase separation can be assumed to be governed by the curvature effect [33]. On the other hand, after complete phase separation of systems AOT/nonionics/IPM/water with $X_{nonionic} \geq X_{nonionic,max}$, addition of Sudan IV made both the phases to turn red, whereas addition of Eosin Blue turned the lower phase violet keeping the upper phase colourless. This indicates that the upper phase is a pure oil phase in equilibrium with the lower microemulsion phase (Winsor I type). Thus for these systems phase separation can be assumed to be governed by the interdroplet interaction phenomenon [33]. Hence in the solubilization capacity versus X_{Brij} profile (Fig. 1), the ascending curve can be identified as the R_0 branch (the curvature branch), whereas the descending curve as the R_c branch (interdroplet interaction branch). The maximization in solubilization capacity for these mixed systems can be explained according to the model proposed by Shah and coworkers [31–33] in the subsequent section.

For a mixed surfactant reverse micellar system, the effective packing parameter (P_{eff}) follows the additive relation [56]:

$$P_{eff} = [(xv/al)_A + (xv/al)_B]/(x_A + x_B) \quad (1)$$

where x_A and x_B are the mole fractions of surfactant A and B in the mixture, respectively. Nonionic surfactants have larger head group area than AOT [57], and thus on mixing Brijs with AOT, P_{eff} is decreased owing to the increase in 'a', which in turn increases the natural radius of curvature (R). Thus AOT/Brij/IPM reveres micelles can accommodate more water than the AOT/IPM reverse micelles, and with increasing $X_{nonionic}$, solubilization capacity of the mixed system increased. But with increasing the droplet size, interdroplet

interaction also increases, and at a certain droplet radius, R_c (the critical radius of curvature) interdroplet interaction starts governing the solubilization behavior and the fluid interfaces can coalesce in order to break the monophasic system into two distinct phases. Thus beyond R_c, addition of nonionic surfactant decreased the solubilization capacity. For all these mixed systems, the ascending curve in the solubilization capacity—$X_{nonionic}$ profile, is governed by the curvature effect due to the rigidity of the interface and the descending curve is governed by the interdroplet interaction effect.

Nazario et al. [58] showed that in AOT/C_iE_j (where i is the number of carbon atoms in the hydrophobic part and j the number of EO chains in the hydrophilic moiety of the nonionic surfactant) mixed surfactant reverse micellar systems stabilized in hydrocarbon oils, the added nonionic surfactant resides at the interfacial region, thereby increasing the droplet radius. In the present systems, the added nonionic surfactants (Brijs) can also be assumed to be preferentially adsorbed at the AOT/IPM interface, and according to Eq. (1), addition of nonionic surfactant decreases P_{eff} and thereby increases the radius of curvature. Larger is the area of polar headgroup 'a' of nonionic surfactants, lower is the value of P_{eff} and hence higher is the value of R at a fixed $X_{nonionic}$. Brij-35 and Brij-58 have 23 and 20 POE chains, respectively, in their headgroups and thus for AOT/Brij-35 and AOT/Brij-58 blended systems, R reached the value of R_c at a relatively lower $X_{nonionic}$ (=0.05). On the other hand, Brij-30, Brij-52 and Brij-56 have 4, 2 and 10 POE chains, respectively, in their polar headgroups and when blended with AOT produced solubilization maxima at relatively higher $X_{nonionic}$ (=0.2, 0.3 and 0.1, respectively). Thus the appearance of maximum in solubilization capacity ($X_{nonionic,max}$) can be inferred to be a function of the area/size of head group of the nonionic surfactants. Brij-76 has equal number of POE chains (10) with that of Brij-56 but 2 more alkyl chains in its hydrophobic moiety in comparison to that of Brij-56 (16 alkyl chains). It has been observed that AOT/Brij-76 blend exhibited a higher solubilization maximum ($\omega_{0,max}$, 35.8) at a lower $X_{nonionic} = 0.05$, whereas that of AOT/Brij-56 blend showed $\omega_{0,max}$ (30.0) at a higher $X_{nonionic,max}$ is 0.1. Thus it can be concluded that the magnitude of both $X_{nonionic,max}$ and $\omega_{0,max}$ does not follow a very straight forward mechanism, instead it is a complex phenomenon involving many factors (e.g. nature of the nonionic surfactant, physicochemical characteristics of oil, external environment, etc.) that modify the interfacial configuration.

We studied the solubilization behavior of AOT/Tween-20 and Tween-40 blended systems in IPM with total surfactant concentration of 0.1 mol dm^{-3}. The solubilization maximum was observed at $X_{Tween} = 0.05$ with corresponding $\omega_{0,max}$ values of 27.3 and 30.0, respectively (Table 1) (figure not shown). Tweens are ethoxylated derivatives of sorbitan esters in which the substitution of the hydroxyl groups on the sorbitan ring with polyoxyethylene groups makes the surfactants hydrophilic with large head group area (HLB values of Tween-20 and 40 are 16.7 and 15.6 respectively, comparable to that of Brij-58 and Brij-35 as mentioned earlier). The solubilization behavior of these systems has also been observed to be identical to that of the AOT/Bri-35 and AOT/Brij-58 blended systems.

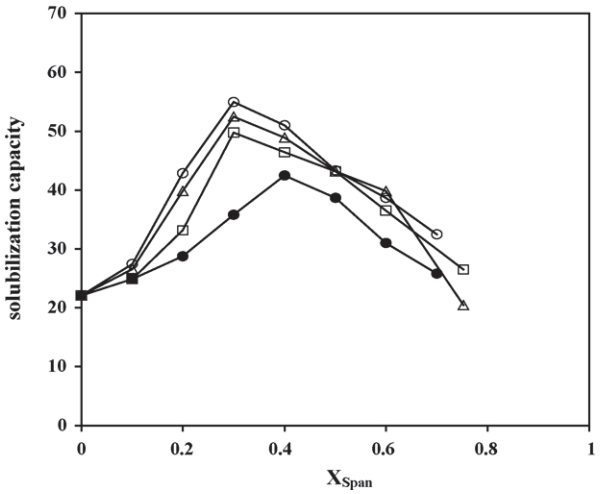

Fig. 2. Solubilization capacity of water in AOT/Span/IPM reverse micellar system at 303 K with total surfactant concentration 0.1 mol dm^{-3} in oil: (●) Span-20; (□) Span-40; (△) Span-60; (◯) Span-80.

Four different Spans (viz. Span-20, Span-40, Span-60 and Span-80) (lipophilic nonionic surfactants, sorbitan fatty acid esters) were blended with AOT in IPM with total surfactant concentration fixed at 0.1 mol dm^{-3} and $\omega_{0,max}$ were determined [Fig. 2]. The Spans have identical polar head group (sorbitan esters) but they differ only in the hydrophobic moiety i.e. in terms of their hydrocarbon chain length. $\omega_{0,max}$ was obtained at $X_{nonionic,max} = 0.4$ for the AOT/Span-20 blend, whereas for the other three blends $\omega_{0,max}$ were obtained at $X_{nonionic,max} = 0.3$. Unlike other nonionic surfactants, Spans do not contain any POE chain. Span-20 has the smallest hydrocarbon tail part (lauric acid side chain on the sorbitan ring) and its HLB value is 8.6. Span-20 is expected to be the most polar compared to Span-40, Span-60 and Span-80, whose HLB values are 6.7, 4.7 and 4.3, respectively. So for the AOT/Span-20 blend producing $\omega_{0,max}$ at a higher $X_{nonionic,max}$ than the other three blends is not consistent with other nonionic surfactants containing EO chains. Since the hydrophilic portion of all the surfactants are similar, the interactions between the fatty acid portions may be the main contributor to the difference in the interfacial elasticities as a consequence of interfacial packing [59]. However, the $\omega_{0,max}$ value increased with increasing hydrophobicity of the tail part of the Spans. The order of $\omega_{0,max}$ values for the Span series is as follows: Span-80 (55.0) > Span-60 (52.5) > Span-40 (50.0) > Span-20 (42.4). Similar observations have been reported by Hou and Shah [33] for AOT/Span-20, Span-40, Span-60/hexadecane/water system.

3.2. Effect of NaCl

The maximum in solubilization capacity of water in reverse micelle is observed as a result of compromise between

two effects (on the curvature of the interface and the attraction among the droplets). As salinity in w/o microemulsions is reported to affect the attractive interaction among the droplets by making the interfacial layer more rigid due to the close packing of polar groups, hence the effect of [NaCl] on the solubilization behavior in mixed reverse micellar systems would be worth while.

3.3. AOT/nonionics/IPM/NaCl (aqueous) at $X_{nonionic} = 0.1$

The AOT/IPM/water (aqueous NaCl) system was observed to show a little increase in the ω_{max} [molar ratio of water (aqueous NaCl) to surfactant(s), 26.5] compared to the aqueous system ($\omega_0 = 22$) at a NaCl concentration of 0.02 mol dm^{-3}. The solubilization capacity of aqueous NaCl in mixed reverse micellar systems, AOT/nonionic(s) in IPM with total surfactant concentration of 0.1 mol dm^{-3} in oil and at $X_{nonionic} = 0.1$ at 303 K has been represented in Fig. 3A (for Brij series) and B (for Spans and Tweens). For all the AOT/Brijs, Tweens, Spans blended systems at the studied composition, solubilization capacity passed through a maximum at a threshold NaCl concentration, $[NaCl]_{max}$. It was further observed that ω_{max} shifted towards a higher concentration of NaCl with the increase in hydrophilicity of the nonionic surfactant depending upon the type and head group configuration of the nonionic surfactants. The maximum solubilization capacity of water ($\omega_{0,max}$), NaCl (ω_{max}) and the corresponding $[NaCl]_{max}$ in IPM based systems are presented in Table 2. From Table 2 it has also been evidenced that for the AOT/nonionic blends with larger polar head (viz. AOT/Brij-35, AOT/Brij-56, AOT/Brij-58, AOT/Brij-76, AOT/Tweens), ω_{max} value increased many fold in comparison to water, whereas for blends with smaller or different configuration of polar head group (viz. AOT/Brij-52, AOT/Brij-30, AOT/Spans), the increase was marginal. Furthermore, lower $[NaCl]_{max}$ were obtained for mixed systems comprising of nonionic surfactants with smaller head group area/configuration. This result is consistent with earlier works [49] for mixed reverse micellar systems containing Brijs (Brij-30, Brij-52, Brij-56, Brij-58) blends with AOT in hydrocarbon oils (cyclohexane, *n*-hexane, *n*-heptane, *n*-octane and *iso*-octane).

Table 2
Solubilization of NaCl (ω_{max}) in mixed reverse micellar systems stabilized by AOT and different nonionic surfactants in IPM with $[S_T] = 0.1$ mol dm^{-3} and $X_{nonionic} = 0.1$ at 303 K

Nonionic surfactant	$\omega_{0,max}$	$[NaCl]_{max}$	ω_{max}
Brij-30	27.5	0.075	36.5
Brij-35	16.0	0.4	82.0
Brij-52	25.0	0.0625	31.0
Brij-56	30.0	0.1	70.0
Brij-58	21.0	0.4	50.0
Brij-76	27.7	0.125	106.0
Tween-20	25.0	0.15	55.0
Tween-40	25.5	0.15	84.0
Span-20	24.0	0.0625	29.0
Span-80	23.0	0.0625	29.0

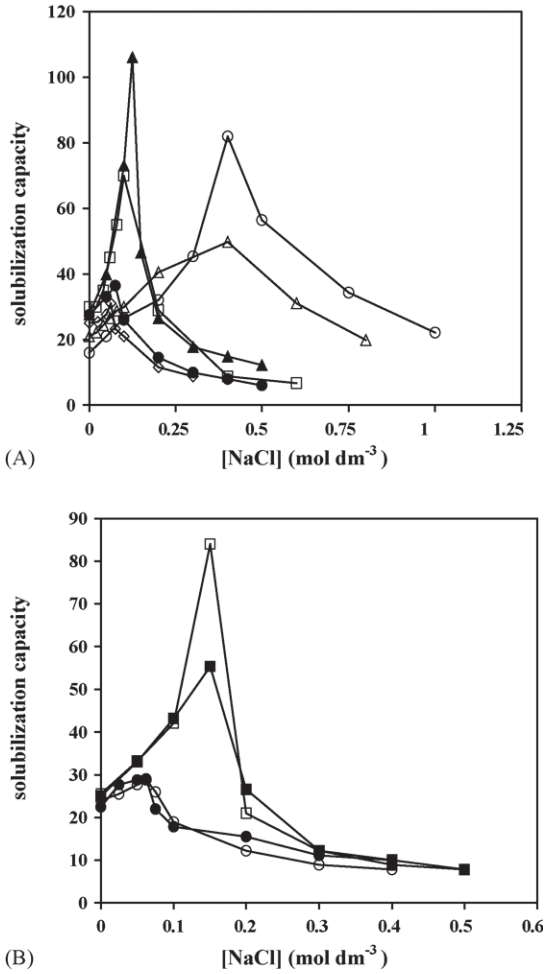

Fig. 3. Solubilization of aqueous NaCl in AOT/nonionic/IPM reverse micellar system at 303 K with surfactant concentration of 0.1 mol dm^{-3} in oil and $X_{nonionic} = 0.1$. The nonionic surfactants used: (A)—(●) Brij-30; (○) Brij-35; (■) Brij-52; (△) Brij-56; (▲) Brij-58; (□) Brij-76; (B)—(■) Tween-20; (□) Tween-40; (○) Span-20; (●) Span-80.

In order to gain more insight to the understanding of the solubilization phenomenon in presence of NaCl, composition of the systems (i.e. $X_{nonionic}$) were varied in mixed reverse micelles and the results are presented in subsequent section.

3.4. AOT/nonionics/NaCl (aqueous) in IPM at different compositions of the nonionics

The effect of NaCl on the solubilization capacity of AOT/Brijs blended systems in IPM (AOT/Brij-52, Brij-56 and Brij-58) with total surfactant concentration of 0.1 mol dm^{-3} and at different $X_{nonionic}$ values, which also includes the $X_{nonionic,max}$ has been studied. A representative Fig. 4 is depicted for AOT/Brij58 blended system. It was observed that solubilization capacity passed through a maximum (ω_{max}, 70.0) at $[NaCl]_{max} = 0.15$ mol dm^{-3} at $X_{nonionic,max} = 0.05$. Further increase in $X_{nonionic}$ (=0.1), de-

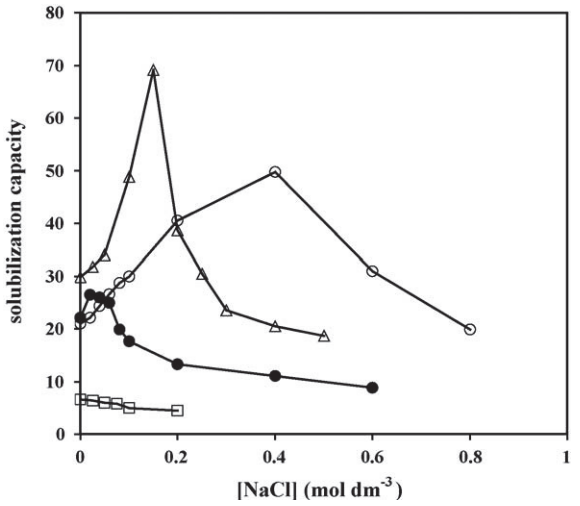

Fig. 4. Solubilization of aqueous NaCl in AOT/Brij-58/IPM reverse micellar system at 303 K with surfactant concentration of 0.1 mol dm^{-3} in oil with $X_{\text{Brij-58}} = 0$ (●); 0.05 (△); 0.1 (◯); 0.3 (□). X represents mole fraction of the respective nonionic surfactant.

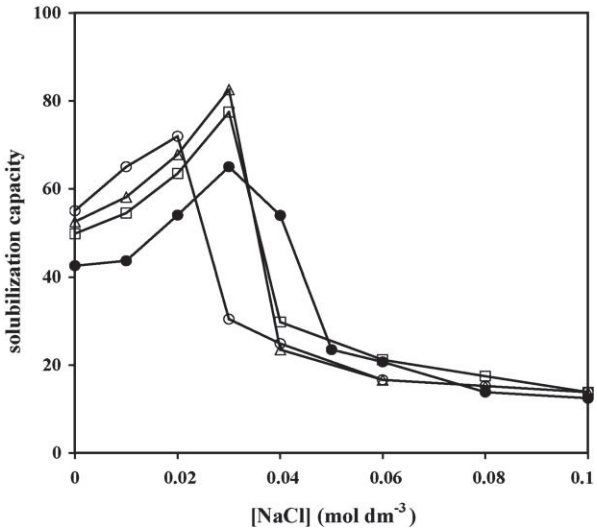

Fig. 5. Solubilization of aqueous NaCl in AOT/Span/IPM reverse micellar system at 303 K with surfactant concentration of 0.1 mol dm^{-3} in oil: (●) Span-20 ($X = 0.4$); (□) Span-40 ($X = 0.3$); (△) Span-60 ($X = 0.3$); (◯) Span-80 ($X = 0.3$).

creased ω_{max} (50.0) in presence of NaCl, and the corresponding $[NaCl]_{max}$ was found to be 0.4 mol dm^{-3}. At $X_{\text{nonionic}} = 0.3$ ($>X_{\text{nonionic,max}}$), solubilization was observed to be very low ($\omega_{max} \sim 6.0$). For the blend AOT/Brij-56, at $X_{\text{nonionic,max}} = 0.1$, the solubilization capacity passed through a maximum (ω_{max}, 70.0) at $[NaCl]_{max} = 0.1$ mol dm^{-3}, whereas for the composition $X_{\text{nonionic}} = 0.3$, solubilization was poorly dependent on [NaCl], and remained almost unchanged with increasing [NaCl] (figure not shown). An interesting point may be noted that the effect of [NaCl] on both these systems at $X_{\text{nonionic}} = 0.3$ was so insignificant that the curves lied below the AOT/IPM/NaCl (aq.) system. For AOT/Brij-52 blended system, at $X_{\text{nonionic}} = 0.1$ ($<X_{\text{nonionic,max}}$), solubilization capacity passed through a maximum (ω_{max}, 34.0) at $[NaCl]_{max} = 0.04$ mol dm^{-3}. At $X_{\text{nonionic,max}} = 0.3$, a similar trend was observed, with corresponding ω_{max}, 64 and $[NaCl]_{max}$ of 0.02 mol dm^{-3} (figure not shown). For all these mixed systems, ω_{max} has been obtained at the corresponding $X_{\text{nonionic,max}}$ i.e. further enhancement in solubilization of NaCl (aq.) was observed at this composition. ω_{max} values are comparable for these mixed reverse micelles, but $[NaCl]_{max}$ depends on the content of POE chains in the nonionic surfactant. Smaller the POE chain, lower $[NaCl]_{max}$ was required to attain ω_{max}.

Solubilization capacity of AOT/Span (20, 40, 60, 80)/IPM/aq. NaCl systems with total surfactant concentration 0.1 mol dm^{-3} at $X_{\text{nonionic,max}}$ has been presented in Fig. 5. It showed maximum in the solubilization capacity-[NaCl] profile for all these systems. For the AOT/Span-80 system, ω_{max} (72.0) was obtained at $[NaCl]_{max} = 0.02$ mol dm^{-3}, whereas for the other three systems (Span-20, Span-40 and Span-60), $[NaCl]_{max}$ were obtained at 0.03 mol dm^{-3} with ω_{max} values (65, 77.4 and 82.5 for Span-20, 40, 60, respectively). It may be noted that the interfacial behavior of these surfactants varied as a result of difference in molecular structure and hydrophobicity. All these aspects are expected to vary in presence of NaCl. It has been reported earlier that interfacial elasticity of Span-20/hydrocarbon oil/water system increases with increasing [NaCl] and then decreases with further increase in [NaCl] [59]. The initial increase in elasticity may be attributed to the salting out of the polar head group of Span-20 from the aqueous phase, resulting in enhanced interfacial packing which in turn results in an increased solubilization. The reduced partitioning of Span molecules from the oil to the aqueous phase may also attribute to this phenomenon. The reduced interaction of the polar hydrophilic head group with the aqueous phase at a higher [NaCl] may induce the decrease of solubilization beyond the maximum. The same argument holds good for the other AOT/Span mixed surfactant systems. It may also be noted that Span-80 is the least polar surfactant among the studied Spans, and hence least amount of NaCl was required to salt out the polar head group and bring about the solubilization maximum.

It can be inferred from these results that both EO chain length (or size/configuration of the polar group) and hydrophobic moiety in nonionic surfactants and their contents (X_{nonionic}) play significant roles to determine both ω_{max} and $[NaCl]_{max}$.

The solubilization maximum obtained in NaCl solution can be explained on the basis of salting in and salting out process [33,34,50,60]. Addition of electrolyte (NaCl) can expel part of the AOT molecules from the aqueous phase to the organic phase to form reverse micelle and hence increases solubilization. Addition of electrolyte decreases the interaction among the droplets by making the interfacial layer more rigid. This in turn increases solubilization. At a higher concentration of NaCl a different phenomenon overcomes this effect. Addition of NaCl decreases the thickness of the electrical double layer of the charged interfacial film and the

effective polar area of the surfactant also decreases. This in turn increases the tendency of the surfactant to form natural negative curvature, which decreases the solubilization. For blends containing nonionic surfactants with larger polar group, the effective polar area of the surfactant at the interface is larger and hence higher concentration of NaCl is required to decrease the effective polar area of the surfactant at the interface. Hence $[NaCl]_{max}$ was high for blends containing nonionic surfactants with large polar head groups. In an AOT based system, the optimum NaCl concentration can be viewed as the concentration of salt just necessary so that the range of electrostatic interaction becomes such that neighboring AOT polar head groups totally ignore each other [61]. It was proposed that the Debye screening length (K^{-1}) would become smaller than the average inter-charge distance between AOT molecules in the surfactant film at optimum salinity. When K^{-1} would be larger than the inter-charge distance, electrostatic repulsion between AOT polar heads would give enough flexibility in the surfactant film for the droplets to be attractive. It is known that K^2 is inversely proportional to ε^{-1}, where ε is the dielectric constant of water [62]. For small droplet sizes, ε of water decreases considerably in the vicinity of the charged surface [63]. It has been observed earlier that NaCl affects very weakly the solubilization behavior of AOT/Brij-56 and AOT/Brij-58 blends with $X_{Brij} = 0.3$. It can be noted that with $X_{Brij} = 0.3$, the droplet sizes are very small (due to the small value of ω) and thus the water present in the droplet is in the vicinity of the charged surface, thus has a considerably small ε value, which in turn reduces the effect of NaCl.

3.5. Effect of temperature on solubilization

It is reported that temperature plays a significant role on solubilization behavior of microemulsion systems with special reference to the systems stabilized by nonionic surfactants [64]. The hydrophile–lipophile balance of nonionic surfactant changes dramatically with increasing temperature due to the conformational change in the hydrophilic moiety. Due to dehydration of the oxyethylene group, nonionic surfactants become more lipophilic with increasing temperature [65]. On the other hand, for ionic surfactants, with increasing temperature, the dissociation of ionic group increases and ionic surfactants become more hydrophilic at an elevated temperature [66].

The effect of temperature on the solubilization capacity in anionic, cationic and nonionic microemulsions (in absence and presence of additives) are sparse. Kandori et al. [67] found that the extent of solubilization by AOT is affected markedly with temperature, but hardly affected by Ca and Ba salts of AOT. Kon-No and Kitahara [28] reported that the optimum solubilization temperature (the temperature at which maximum water uptake occurs) became larger upon increasing the alkyl chain length of dodecylammonium carboxylates in benzene solutions. Kon-No and Kitahara [29] and Kizling and Stenius [68] reported that the solubilization

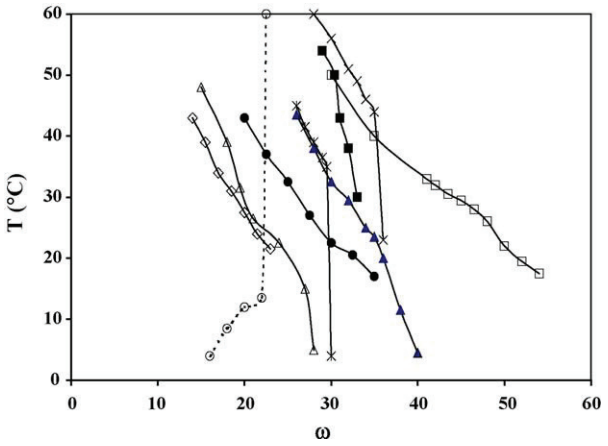

Fig. 6. Temperature induced water solubilization curves for the systems: (◯) AOT; (◇) AOT/Brij-35 ($X = 0.1$); (*) AOT/Brij-58 ($X = 0.05$); (△) AOT/Brij-58 ($X = 0.1$); (▲) AOT/Brij-56 ($X = 0.1$); (×) AOT/Brij-76 ($X = 0.05$); (■) AOT/Brij-30 ($X = 0.2$); (□) AOT/Brij-52 ($X = 0.3$); (●) AOT/Tween-40 ($X = 0.1$) in IPM with total surfactant concentration of 0.1 mol dm^{-3}. X represents mole fraction of the respective nonionic surfactant.

parameters depend exponentially on temperature, electrolyte concentration and EO content of nonionic surfactants for a series of polyoxyethylene ethers (where EO chains were varied from 5 to 10) in tetrachloro ethylene solutions. Kon-No and Kitahara [26,28] further reported that the shifting of solubilization region towards higher or lower temperature in temperature versus [water]/[surfactant] profile, depends on the type of cations or anions of the additives (electrolytes, acids and bases) and also on the charge types of the surfactants used (i.e. dodecylammonium propionate in benzene and AOT in cyclohexane). These results were explained on the basis of DLVO theory, Lewis' acid–base theory as applicable for these systems. Kon-No and Kitahara [26] reported that the solubilization of water changed markedly by mixing two kinds of surfactants, the effect of anionic surfactant (AOT) was found to depend on the structure and type of the nonionic surfactant. For polyoxyethylene (4,6,8,10) nonylphenyl ethers, AOT increased the optimum solubilization temperature of water and broadened the solubilization region. Similar increase in water uptake was observed for the monooleate esters, accompanied by a noticeable decrease in the optimum solubilization temperature.

In the present investigation, ω has been plotted against temperature for AOT/nonionic blended systems stabilized in IPM (in absence and presence of additives) at different compositions in order to underline the stability of the formulations with respect to temperature and can be extended to compare the solubilization capacity of these systems at any particular temperature. The results have been depicted in Figs. 6–10. For the AOT/IPM/water system (with $\omega \leq 22$), the systems were found to be hazy at lower temperatures (up to 13 °C) and as the temperature was increased, the systems became clear. This temperature is referred to as the mixing temperature (temperature at which the components mix together in order to form a clear solution) [69,70]. Thus up to $\omega = 22$, a

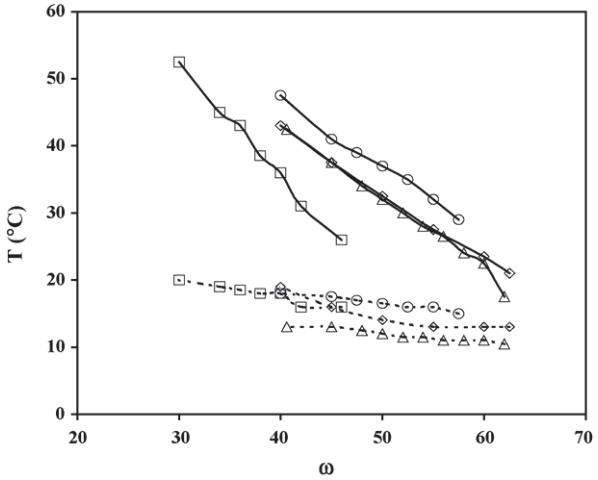

Fig. 7. Temperature induced water solubilization curves for the systems: AOT/Spans/IPM/water with total surfactant concentration of 0.1 mol dm^{-3}: (□) Span-20 (X = 0.4); (△) Span-40 (X = 0.3); (◊) Span-60 (X = 0.3); (◯) Span-80 (X = 0.3). X represents mole fraction of the respective nonionic surfactant.

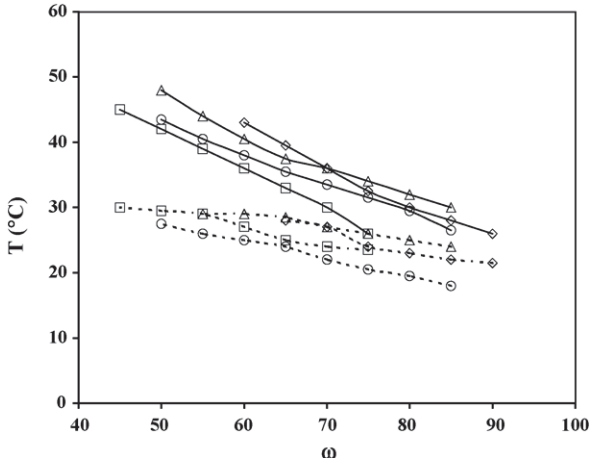

Fig. 9. Temperature induced water solubilization curves for the systems: AOT/Spans/IPM/aqueous NaCl with total surfactant concentration of 0.1 mol dm^{-3}: (□) Span-20 (X = 0.4, [NaCl] = 0.03 mol dm^{-3}); (△) Span-40 (X = 0.3, [NaCl] = 0.03 mol dm^{-3}); (◊) Span-60 (X = 0.3, [NaCl] = 0.03 mol dm^{-3}); (◯) Span-80 (X = 0.3, [NaCl] = 0.02 mol dm^{-3}). X represents mole fraction of the respective nonionic surfactant.

lower solubility curve was obtained for the AOT/IPM/water system (Fig. 6). Each point on this curve indicates the temperature at which a system with fixed ω gets clear. With $\omega > 22$, no clear monophasic region was obtained for this system. However, the systems with $\omega < 22$, exhibited strong temperature resistance and the formulations did not get turbid up to 60 °C. It has been observed earlier that water solubilization in AOT/IPM system is governed by the curvature effect. Thus the AOT coated water droplets in IPM can be viewed as hard spheres which do not interact with each other. Hence increase in temperature can hardly make the droplets to interact and thus the system exhibited high temperature stability. The lower solubility curve corresponded to the mixing temperature and was governed by the water penetration across the interface of the droplets [69,70]. Since the droplets are very rigid such penetration across the droplets is very difficult and hence the lower solubility curve appeared. When nonionic surfactants (Brij-30, Brij-35, Brij-52, Brij-56, Brij-58, Brij-76, Tween-40 and Spans) were blended with AOT in IPM with $X_{\text{nonionic}} \geq X_{\text{nonionic,max}}$, the systems exhibited strong dependence on temperature. The lower solubility curve disappeared, instead upper solubilization curve appeared for the AOT/Brijs and AOT/Tween mixed systems (Fig. 6). The upper solubilization curves correspond to the stability of the mixed reverse micellar systems with respect to temperature. It has been identified earlier that the solubilization behavior of AOT/Brijs blends in IPM at $X_{\text{nonionic}} \geq X_{\text{nonionic,max}}$ is governed by the interdroplet interaction effect using dye

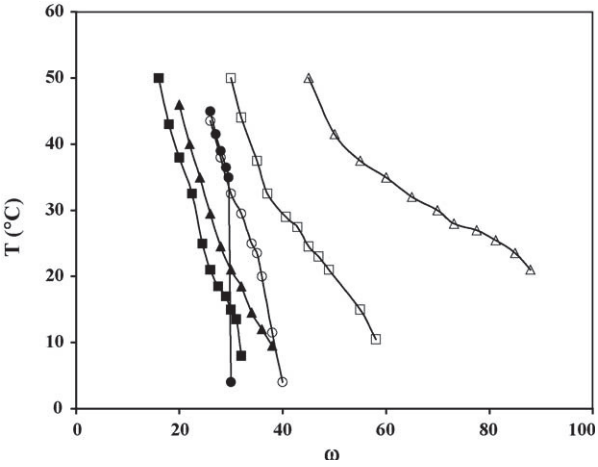

Fig. 8. Temperature induced water solubilization curves for the systems: AOT/Brijs/IPM/water (or aqueous NaCl) with total surfactant concentration of 0.1 mol dm^{-3} and X_{Brij} = 0.1. The open symbols represent AOT/Brij-56 systems and the filled symbols represent AOT/Bri-58 systems. (◯) Water; (□) 0.05 mol dm^{-3} NaCl; (△) 0.1 mol dm^{-3} NaCl.

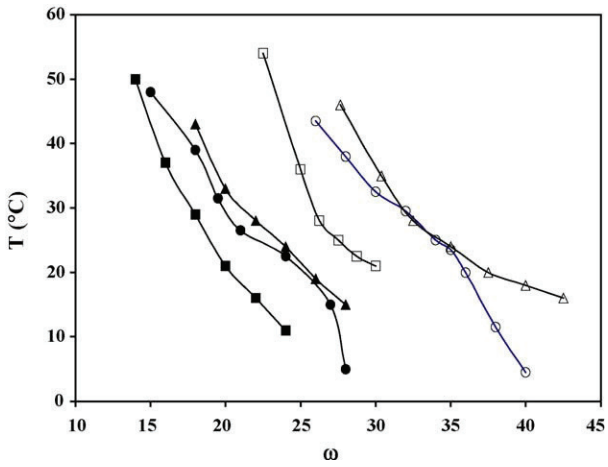

Fig. 10. Temperature induced water solubilization curves for the systems: AOT/Brijs/IPM/water in presence of 0.2 mol dm^{-3} urea and 1% cholesterol with total surfactant concentration of 0.1 mol dm^{-3} at X_{Brij} = 0.1. The open symbols represent AOT/Brij-56 systems and the filled symbols represent AOT/Bri-58 systems. (◯) No additive; (□) urea; (△) cholesterol.

solubilization method. The droplets at these compositions are fluid and can easily interact with each other, coalesce and can exchange materials. However, increasing temperature makes the droplets to interact more rapidly and phase separation occurred due to the coalescence of the droplets. Each point on the solubilization curve denotes the temperature at a fixed ω, the mixed reverse micellar system gets destabilized and phase separation occurred. The disappearance of the lower solubility curve can be correlated with the enhanced solubilization of water into the droplet cores owing to the fluid interface, which in turn reduced the mixing temperature below the experimental range. It can be observed from the solubilization–temperature profile that as ω was increased, the phase separation temperature decreased. This can be argued as follows; as ω increases, radius of the droplets increases linearly [33] and larger is the droplet size greater is the interaction among them. Hence, higher is the probability of the droplets to coalesce followed by phase separation. Thus with increasing ω, phase separation occurred at lower temperatures. It can also be noted that the AOT/Brij-58 curves lie below the AOT/Brij-56 curves at a comparable mole fraction of nonionic surfactant, X_{Brij}. This observation can be attributed due to the larger head group size of Brij-58 in comparison to Brij-56, and is supported from the report of Liu et al. [57]. They have shown with the help of DLS measurements that the droplet size increased with increasing polar head group size of the nonionic surfactants for an AOT/Brij/heptane mixed reverse micellar system. Also it follows from Eq. (1) that the decrease in 'a' decreases P_{eff}, which in turn increases droplet radius. Hence, larger droplet size enhances the possibility of greater interaction of droplets and the system becomes more prone to temperature induced phase separation. Further increase in X_{Brij} made the formulations less stable. Actually, size of the droplets in AOT/Brij blended systems in IPM is increased further due to the increased content of the nonionic surfactant (X_{Brij}) [55,57], which in turn decreased their thermal stability.

To study the effect of temperature on the solubilization behavior of systems lying in the R_0 branch of the solubilization profile, temperature dependent solubilization capacity of AOT/Brij-52 and Span-40 systems with $X_{\text{nonionic}} = 0.1$ ($< X_{\text{nonionic,max}}$) was studied. It was found that for both these systems, lower solubility curve was present, whereas no upper solubilization curve was obtained within the experimental range (figure not shown). At this nonionic content both the systems have rigid interfaces, which in turn made them resistant towards temperature.

Temperature induced solubilization curves were obtained for the systems AOT/Spans/IPM/water with four different Spans (Span-20, 40, 60, 80) at $X_{\text{nonionic,max}}$ (=0.4 for Span-20 and $X = 0.3$ for Span-40, 60 and 80). Both lower solubility curves and upper solubilization curves were observed for all these systems (Fig. 7). In the lower solubility curve, the AOT/Span-40 system was found to be at the bottom, whereas AOT/Span-80 system at the top. The AOT/Span-20 and AOT/Span-60 curves were closely placed. For the upper solubilization curves, it was found that the AOT/Span-20/IPM/water curve was the lowest lying curve, whereas the AOT/Span-80/IPM/water curve was the highest lying curve. The other two curves lied in between these two curves. The temperature stability at the same ω decreased in the order, AOT/Span-80 > AOT/Span-60 > AOT/Span-40 > AOT/Span-20. Span-20 possesses the smallest hydrophobic tail among the studied Spans, and therefore oil can penetrate more into the interface making the interface more fluid and hence reduces the thermal stability.

Temperature dependence on the solubilization behavior of the system AOT/nonionic (Brij-56 and Brij-58)/IPM at fixed $X_{\text{nonionic}} = 0.05$, 0.1, respectively, in presence of NaCl with varying concentrations (0.05, 0.1, 0.15 mol dm^{-3}) was examined and is depicted in Fig. 8. It can be noted that for AOT/Brij-58 and AOT/Brij-56 blended systems solubilization maximum were obtained at $X_{\text{Brij}} = 0.05$ and 0.1, respectively, and at these compositions solubilization behavior is governed by the interdroplet interaction for both these systems. For both the mixed surfactant systems, the solubilization curves were shifted towards higher temperature with respect to the aqueous systems. As mentioned earlier, NaCl makes the interface more rigid by shielding the charged headgroup and thereby decreased the interaction among the droplets and makes the formulations less susceptible towards temperature. Effect of NaCl on temperature induced solubilization behavior of AOT/Spans/IPM reverse micellar systems were also carried out with four different Spans at corresponding $X_{\text{nonionic,max}}$ and $[\text{NaCl}]_{\text{max}}$. It was found that for all these systems the lower solubility curves were shifted towards higher temperature in comparison to the aqueous systems, indicating an increase of mixing temperature in presence of NaCl (Fig. 9). However, the upper solubilization curve did not shift considerably in comparison to the aqueous systems. The AOT/Span-20 solubilization curve lied at the bottom as was observed in the aqueous system, and the sequence of the thermal stability for other AOT/Spans followed the same order (as in the case of aqueous systems) with exception for AOT/Span-80 blended system.

Temperature induced solubilization behavior of AOT/Brij-56 and Brij-58 blended systems in IPM oil (with total surfactant concentration of 0.1 mol dm^{-3} at $X_{\text{Brij}} = 0.1$) has been carried out in presence of 0.2 mol dm^{-3} urea and 1% cholesterol, and the solubilization curves are represented in Fig. 10. It was observed that at a fixed ω, urea decreased the thermal stability of the system as compared to the system without additive, whereas cholesterol increased it. It can also be observed that at any particular temperature, cholesterol increased the solubilization capacity, whereas urea decreased it with respect to the system without additive for both the blended systems. However, the solubilization curves of AOT/Brij-58 blended systems lie below that of the AOT/Brij-56 blended systems for both the additives. Cholesterol is known to form hydrogen bond with the hydrophilic part of the surfactant and make the droplets more rigid [69,71,72]. Water photon NMR relaxation measurements has established that

the intermolecular hydrogen bonding between the 3β-OH group of cholesterol and the carbonyl ester of AOT is responsible for the decrease in hydrophilicity of the surfactant molecule in presence of cholesterol [73]. Thus in the presence of cholesterol, the surfactant monolayer of the droplets become more rigid. This fact has also been supported by the work of Mukhopadhay et al. [71] by fluorescence depolarization measurements. In addition, such type of bonding between nonionics and cholesterol cannot be ruled out. All these factors may shift the solubilization curve towards a higher temperature. On the other hand urea is known to interact with the head group of surfactant present at the interface and can also act as a structure breaker. It is reported that preferential solubilization of urea at the micellar interface increases the interfacial flexibility and enhances the attractive potential among micelles [74]. Potential solvation of the surfactant headgroups by urea results in an increase in the monomer i.e. degree of dissociation, which leads to an increase in the area per headgroup of the system [75]. This in turn increases droplet size of reverse micellar systems in presence of urea. It has been shown by Farnando and Politi et al. [75] that incorporation of urea in AOT/hexane/water reverse micellar system increased droplet size. This explains the present increased fluidity of the interface constituted by AOT/Brijs in IPM in presence of urea and consequently solubilization curve was shifted to a lower temperature.

3.6. Thermodynamics of desolubilization of water in mixed reverse micellar systems

The mechanism of solubilization of water was inferred from the measurements of the differential heat of solubilization (ΔH_s) for AOT in various nonpolar solvents (cyclohexane, *n*-heptane, tetrachloro ethylene and benzene) using the Clapeyron–Clausius equation from the temperature dependence of the vapour pressure of solubilized water by Kon-No and Kitahara [30]. The value of ΔH_s decreases rapidly up to the molar ratio ([water]/[surfactant]) of unity and subsequently approaches the heat of condensation of water ($10.8\,\text{kcal mol}^{-1}$). These results indicated that the water molecules solubilized initially interact strongly with the ionic part of the surfactant by ion–dipole interaction, and the water molecules solubilized later interact with water itself by hydrogen bonding (similar to the condensation of water) that exists as free water in the micelle. The poorer were the solvents, larger were the ΔH_s values at the initial stage of solubilization. This behavior of solubilized water has been ascertained by the density measurements of water [76]. They further reported [77] that the change in ΔH_s as a function of the molar ratios of water to polyoxyethylene (average number of EO units: 2.5, 4.1, 5.7, 6.3) 2-(1,3-dihexaoxypropyl) ethers in benzene. The undulating nature of ΔH_s was characterized by an increase in the molar ratio of water and with the increase in the oxyethylene chain length of surfactants. However, systematic trend (i.e. a minimum in ΔH_s was observed) at $n = 6.3$. The results indicated that the interaction between the water molecules and ether oxygens of the oxyethylene chain of the surfactant to be of hydrogen bonding type.

In the present study, it has been observed that the upper solubilization curve appeared in the ω versus T profile for AOT/nonionics/IPM/water systems lying in the R_c branch (i.e. at $X_{\text{nonionic}} \geq X_{\text{nonionic,max}}$), whereas such curve was absent for systems lying in the R_0 branch (i.e. at $X_{\text{nonionic}} < X_{\text{nonionic,max}}$). Appearance of the upper solubilization curve indicates the coalescence of w/o droplets owing to their increased thermal motion upon increasing temperature. Any point at the upper solubilization curve denotes the optimum solubilization temperature (T_U) (represented as phase separation temperature earlier) of a certain composition of surfactant(s)/oil/water system. If temperature is increased further, the clear composition separates out into two distinct phases. Dye solubilization study indicates that the lower phase is an o/w microemulsion phase in equilibrium with an excess oil phase. Increased temperature induces increased thermal motion of the surfactant coated water droplets immersed in oil continuum, and fusion of droplets gives rise to instability of the formulation, which follows the formation of a microemulsion phase with oil droplets immersed in water continuum and a subsequent expulsion of the excess oil as a distinct phase (Winsor I system). If the water present in the microemulsion phase can be assumed to be equivalent to bulk water, then at the phase separation temperature (herein upper solubilization temperature, T_U) an equilibrium exists between the bulk water and the entrapped water of the droplets. The equilibrium attains the form:

$$\text{Water}_{\text{droplet}} \rightleftharpoons \text{Water}_{\text{bulk}}(\text{at } T_U) \tag{2}$$

The corresponding condition for equilibrium can be written as:

$$\mu_w(\text{droplet}) = \mu_w(\text{bulk}) \tag{3}$$

where μ_w(droplet) is the chemical potential of water entrapped in w/o droplets and μ_w(bulk) the chemical potential of water in bulk. If bulk water can be assumed to be in its standard state (i.e. in pure state), then Eq. (1) can be written in the form:

$$\mu_w^0(\text{droplet}) + RT_U \ln X_w = \mu_w^0(\text{bulk}) \tag{4}$$

where μ_w^0(droplet) is the chemical potential of water entrapped in droplets in its standard state, μ_w^0(bulk) is that of bulk water, X_w the mole fraction of water in the droplets (assuming equal to the activity of water) and R the universal gas constant. Eq. (3) takes up the form:

$$\mu_w^0(\text{bulk}) - \mu_w^0(\text{droplet}) = RT_U \ln X_w,$$
$$\Delta\bar{G}^\circ = RT_U \ln X_w \tag{5}$$

where $\Delta\bar{G}^\circ$ is the standard molar Gibbs free energy change associated with the desolubilization process.

The corresponding standard enthalpy change ($\Delta\bar{H}^\circ$) of the process can be determined using the Gibbs Helmoltz

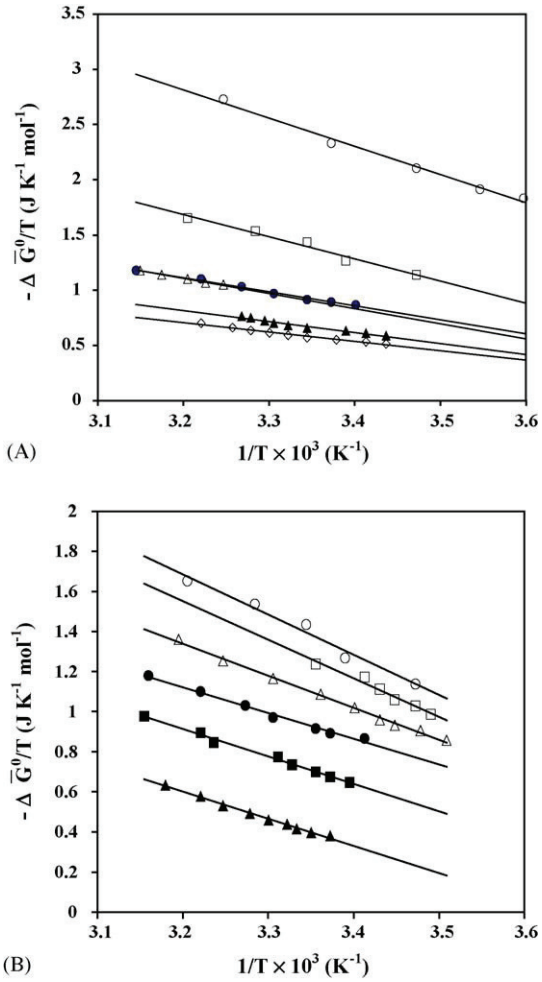

Fig. 11. (A) $-\Delta\bar{G}^\circ/T$ against $1/T$ plot for the system AOT/nonionic/IPM/water with overall surfactant concentration of 0.1 mol dm^{-3} in oil: (◯) AOT/Brij-58 (X=0.2); (□) AOT/Bri-58 (X=0.1); (△) AOT/Brij-58 (X=0.05); (●) AOT/Brij-56 (X=0.1); (▲) AOT/Brij-52 (X=0.3); (◊) AOT/Span-40 (X=0.3). (B) $-\Delta\bar{G}^\circ/T$ against $1/T$ plot for the system AOT/Brijs/IPM/water (or aqueous NaCl) with overall surfactant concentration of 0.1 mol dm^{-3} in oil. Filled symbols represent AOT/Brij-58 systems and open symbols represent AOT/Brij-56 systems. (◯) water; (□) 0.05 mol dm^{-3} NaCl; (△) 0.1 mol dm^{-3} NaCl.

equation:

$$[\partial(\Delta\bar{G}^\circ/T)/\partial(1/T)] = \Delta\bar{H}^\circ \quad (6)$$

The standard entropy of the desolubilization process can be obtained from the relation:

$$\Delta\bar{S}^\circ = (\Delta\bar{H}^\circ - \Delta\bar{G}^\circ)/T_U \quad (7)$$

In the present study, we measured the T_U of mixed systems having different compositions (X_W) and calculated $\Delta\bar{G}^\circ$ from Eq. (5). Straight lines with good linear fits were obtained when $-\Delta\bar{G}^\circ/T$ were plotted against $1/T$ for different mixed systems (in absence and presence of additives) (Fig. 11) and the $\Delta\bar{H}^\circ$ values were obtained from the corresponding slopes. The $\Delta\bar{H}^\circ$ and $\Delta\bar{S}^\circ$ values were presented in Table 3.

The present model can be viewed as a very simplified picture of a complex phenomenon of phase separation. As mentioned earlier, it involves various factors like the type, content and configuration of the nonionic surfactant, different physical and chemical properties of the oil (e.g. molar volume, molecular structure, viscosity, polarity, etc.), presence of additives etc. Hou and Shah [33] developed an equation for the estimation of free energy of mixing of water droplets (assuming them to be of hard sphere type) in oil continuum. This equation involved certain parameters, which are very difficult to estimate experimentally. It has been mentioned earlier that our model is based on the results obtained from dye solubilization method that the upper phase contains no water and the lower phase is a water continuous microemulsion, wherein the water present has a close resemblance with that of the bulk water. In actual system, the upper phase (oleic phase) may contain certain amount of surfactant dissolved in it, and hence the possibility of existence of trace amount of water in this phase cannot be ignored (though no colour was developed in this phase upon addition of Eosin Blue). Besides, there are more than one states of water present in the water pool of reverse micelles as evidenced from different experiments [78–81] and there exists equilibrium between the different states of water within the waterpool. In our model, we did not also consider the above mentioned equilibrium while formulating Eq. (2). Furthermore, the water present in the lower phase may contain dispersed surfactant monomers. However, the thermodynamic parameters (free energy, enthalpy and entropy) derived on the basis of this model can account for the solubilization behavior in mixed surfactant systems with these limitations.

It can be observed that all the $\Delta\bar{H}^\circ$ values are positive, which indicates an endothermic desolubilization process i.e. heat is to be supplied from outside in order to induce phase separation. All the $\Delta\bar{S}^\circ$ values were also found to be positive which denotes an entropically favorable desolubilization process. The entrapped water inside the AOT/nonionic film can be assumed to be strongly hydrogen bonded with the polar head groups of both the sulphonic headgroup of AOT and ether oxygen of POE chains of nonionic surfactants. Expulsion of water from the droplet core as bulk water is associated with the breaking of these hydrogen bonds, which makes the associated entropy change positive.

It is evident from Table 3 that both the $\Delta\bar{H}^\circ$ (in the range of 1580–1273 J mol^{-1}) and $\Delta\bar{S}^\circ$ (in the range of 5.7–4.8 J K^{-1} mol^{-1}) for AOT/Brijs and Tweens blends in IPM are comparable at their corresponding composition of $[S_T] = 0.1$ mol dm^{-3} and at $X_{nonionic,max}$ except for the AOT/Brij-30 blend. Similarly such parameters for AOT/Spans blended systems at same composition, $X_{nonionic,max}$ are also comparable, but the value of these parameters ($\Delta\bar{H}^\circ$ in the range of 1073–1250 J mol^{-1} and $\Delta\bar{S}^\circ$ in the range of 4.3–4.7 J K^{-1} mol^{-1}) are somewhat smaller than the previous mixed reverse micelles. These small differences in both these parameters may be attributed due to the basic differences in the configuration of the polar head group

Table 3
Thermodynamic parameters of desolubilization process ($\Delta\bar{H}^\circ$ and $\Delta\bar{S}^\circ$) for different mixed reverse micellar systems with total surfactant concentration of 0.1 mol dm^{-3}

System	$\Delta\bar{H}^\circ$ (J mol^{-1})	$\Delta\bar{S}^\circ$ (J K^{-1} mol^{-1})	Corr. coeff.
AOT/nonionic/IPM/water systems			
AOT/Brij-58/IPM/water, $X_{Brij} = 0.05$ ($X_{Brij\text{-}58,max}$)	1374	5.5	0.9920
AOT/Brij-58/IPM/water, $X_{Brij} = 0.1$	2003	8.1	0.9778
AOT/Brij-58/IPM/water, $X_{Brij} = 0.2$	2563	11.1	0.9915
AOT/Brij-56/IPM/water, $X_{Brij} = 0.05$	623	2.9	0.9955
AOT/Brij-56/IPM/water, $X_{Brij} = 0.1$ ($X_{Brij\text{-}56,max}$)	1275	5.2	0.9928
AOT/Brij-52/IPM/water, X_{Brij}=0.3 ($X_{Brij\text{-}52,max}$)	1351	5.2	0.9936
AOT/Brij-76/IPM/water, $X_{Brij} = 0.05$ ($X_{Brij\text{-}76,max}$)	1237	4.8	0.9976
AOT/Brij-30/IPM/water, $X_{Brij} = 0.2$ ($X_{Brij\text{-}30,max}$)	467	2.5	0.9938
AOT/Brij-35/IPM/water, $X_{Brij\text{-}35} = 0.05$ ($X_{Brij\text{-}35,max}$)	1580	5.7	0.9913
AOT/Brij-35/IPM/water, $X_{Brij\text{-}35} = 0.1$	3177	12.1	0.9933
AOT/Tween-40/IPM/water, $X_{Tween\text{-}40} = 0.05$ ($X_{Tween\text{-}40,max}$)	1402	5.6	0.9928
AOT/Tween-40/IPM/water, $X_{Tween\text{-}40} = 0.1$	2133	8.2	0.9951
AOT/Span-20/IPM/water, $X_{Span} = 0.4$ ($X_{Span\text{-}20,max}$)	1073	4.3	0.9833
AOT/Span-40/IPM/water, $X_{Span} = 0.3$ ($X_{Span\text{-}40,max}$)	1116	4.4	0.9915
AOT/Span-60/IPM/water, $X_{Span} = 0.3$ ($X_{Span\text{-}60,max}$)	1201	4.6	0.9951
AOT/Span-80/IPM/water, $X_{Span} = 0.3$ ($X_{Span\text{-}80,max}$)	1250	4.7	0.9820
In presence of additives			
AOT/Brij-58/IPM/NaCl, $X_{Brij\text{-}58} = 0.05$; [NaCl] = 0.05 mol dm^{-3}	1651	6.3	0.9958
AOT/Brij-58/IPM/NaCl, $X_{Brij\text{-}58} = 0.05$; [NaCl] = 0.1 mol dm^{-3}	1789	6.5	0.9944
AOT/Brij-58/IPM/NaCl, $X_{Brij\text{-}58} = 0.05$; [NaCl] = 0.15 mol dm^{-3}	2142	7.3	0.9903
AOT/Brij-56/IPM/NaCl, $X_{Brij} = 0.1$; [NaCl] = 0.05 mol dm^{-3}	1365	5.3	0.9943
AOT/Brij-56/IPM/NaCl, $X_{Brij} = 0.1$; [NaCl] = 0.1 mol dm^{-3}	1594	5.5	0.9943
AOT/Span-20/IPM/water, $X_{Span} = 0.4$; [NaCl] = 0.03 mol dm^{-3}	1535	5.5	0.9865
AOT/Span-40/IPM/water, $X_{Span} = 0.3$; [NaCl] = 0.03 mol dm^{-3}	1415	5.0	0.9981
AOT/Span-60/IPM/water, $X_{Span} = 0.3$; [NaCl] = 0.03 mol dm^{-3}	948	3.5	0.9984
AOT/Span-80/IPM/water, $X_{Span} = 0.3$; [NaCl] = 0.02 mol dm^{-3}	1598	5.7	0.9953
AOT/Brij-56/IPM/aq. urea, $X_{Brij\text{-}56} = 0.1$; [urea] = 0.2 mol dm^{-3}	1097	4.7	0.9975
AOT/Brij-56/IPM/cholesterol/water $X_{Brij\text{-}56} = 0.1$; [cholesterol] = 1% in oil (w/v)	1155	4.6	0.9878
AOT/Brij-58/IPM/aq. urea, $X_{Brij\text{-}58} = 0.1$; [urea] = 0.2 mol dm^{-3}	1905	8.0	0.9982
AOT/Brij-58/IPM/cholesterol/water, $C_S = 0.1$; $X_{Brij\text{-}58} = 0.1$; [cholesterol] = 1% in oil (w/v)	1850	7.5	0.9934

and hydrophobic moiety of the nonionics. On the whole, both of these parameters ($\Delta\bar{H}^\circ$ and $\Delta\bar{S}^\circ$) are well within the comparable range for AOT/nonionic blends in IPM. It has been mentioned earlier that the solubilization capacity of a mixed system reaches its maximum at $X_{nonionic,max}$ and can accommodate maximum amount of the aqueous phase. From these energetic parameters for desolubilization of water, which was obtained at the maximization of the process, it can be inferred that the existence of an optimum hydrogen bonded network structure of water molecules with the polar head group of the nonionics inside the droplet core. Hence a comparable energy is required to impart disorder into the systems. Thus the energetic parameters corroborates well to the maximization phenomenon of water solubilization capacity in mixed systems as discussed in the previous section. In addition, several factors (for example, the content and configuration of the polar head group of nonionic surfactants, their hydrophobic moiety etc. for a particular oil) determine the value of $\omega_{0,max}$ for these mixed systems. It can be inferred that at the solubilization maximum, contributions of all these factors are optimized in order to attain $\omega_{0,max}$ as revealed from the thermodynamic point of view. It can be also be noted from Table 3 that AOT/Brij-35, Brij-58, Tween-40 blends in IPM have higher $\Delta\bar{H}^\circ$ values compared to the AOT/Brij-56 blend at the comparable composition of $[S_T] = 0.1$ mol dm^{-3} and $X_{nonionic} = 0.1$. The $\Delta\bar{H}^\circ$ values can be correlated with the size of the polar head group of nonionic surfactants in such a way that larger the polar head group, higher is the $\Delta\bar{H}^\circ$ values. It can be argued that nonionic surfactants with large head groups contain more ether oxygen in their head groups, which form stronger hydrogen bond with the entrapped water and hence the desolubilization process would be more endothermic. The same argument holds good for the observed higher $\Delta\bar{S}^\circ$ values for systems with larger head groups, since they form stronger hydrogen bond with water and produces high positive entropy change upon disruption. It has also been observed that both $\Delta\bar{H}^\circ$ and $\Delta\bar{S}^\circ$ increased with increase in $X_{nonionic}$ (beyond $X_{nonionic,max}$) for AOT/Brij-35, Brij-56, Brij-58 and Tween-40 blends in IPM. The increase in $X_{nonionic}$ is associated with an increased number of nonionic surfactants at the interfacial film with polar groups orienting towards the water pool. As a result stronger hydrogen bonding between the polar head groups of the nonionic surfactants and entrapped water which results in higher $\Delta\bar{H}^\circ$ and $\Delta\bar{S}^\circ$ values during desolubilization process.

It can be observed from Table 3 that both the energetic parameters ($\Delta\bar{H}^\circ$ and $\Delta\bar{S}^\circ$) increased with the increase in [NaCl] at the respective fixed compositions (i.e.

with total surfactant concentration of 0.1 mol dm^{-3} and at $X_{\text{Brij-58,max}} = 0.05$ and $X_{\text{Brij-56,max}} = 0.1$) for AOT/Brij blended systems in IPM. The highest values of these parameters were observed at the respective $[\text{NaCl}]_{\text{max}}$ (i.e. at 0.15 and 0.1 mol dm^{-3} NaCl where ω_{max} was obtained for AOT/Brij-58 and AOT/Brij-56 respectively). It can further be noted that both of these parameters have been found to be higher as compared to the corresponding aqueous systems, and the values of AOT/Brij-58 systems are larger than that of AOT/Brij-56 systems. For the AOT/Spans blended system, the $\Delta\bar{H}^{\circ}$ and $\Delta\bar{S}^{\circ}$ values increased in comparison to the aqueous systems at the corresponding $[\text{NaCl}]_{\text{max}}$ (except for the AOT/Span-60 system). From these thermodynamic results, it can be inferred that the presence of NaCl influences the interfacial rigidity and vis-à-vis the interaction among the droplets in these systems. On the other hand, the content, size and configuration of polar head group, hydrophobic moiety of nonionic surfactants played a significant role under this changed environment. As mentioned earlier, incorporation of NaCl makes the interfacial film less flexible by shielding the charge of AOT headgroups and thereby reducing the head group repulsion. This perhaps also makes possibility of the formation of the hydrogen bond between water inside the droplets and the polar interface more feasible, which in turn made the desolubilization process more endothermic. These views corroborate the further maximization of the solubilization capacity of mixed systems in presence of NaCl at their corresponding $X_{\text{nonionic,max}}$ as discussed in previous section. Both urea and cholesterol also increased the $\Delta\bar{H}^{\circ}$ values for AOT/Brij-58 blended systems in comparison to the aqueous system, which can be substantiated due to the ability of these additives to form hydrogen bonds with polar head groups of surfactants and water within the droplets. However, for AOT/Brij-56 blend, these additives decreased $\Delta\bar{H}^{\circ}$ values. In order to underline these unusual behaviors of these additives in thermodynamic study, a more comprehensive study on the solubilization of water in presence of additives, which makes the interface either rigid or flexible, at different temperatures needs to be explored.

4. Conclusions

- Addition of nonionic surfactants (Brijs, Tweens, Spans) into AOT/IPM reverse micellar system enhances the solubilization capacity ($\omega_{0,\text{max}}$) at certain $X_{\text{nonionic,max}}$ depending upon the polar head group and the hydrophobic moiety of the added nonionic surfactants. The ascending curve in the solubilization capacity-X_{nonionic} profile is the R_0 branch (the curvature branch), whereas the descending branch is the R_{c} (interdroplet interaction branch).
- Addition of electrolyte (NaCl) to these mixed systems at $X_{\text{nonionic}} = 0.1$ and at $X_{\text{nonionic,max}}$ increases the solubilization capacity at a maximum (ω_{max}) at a certain NaCl concentration ($[\text{NaCl}]_{\text{max}}$). The magnitude of $[\text{NaCl}]_{\text{max}}$ depends upon the type of the nonionic surfactant.
- AOT/IPM system is strongly temperature insensitive, whereas AOT/nonionic blends in IPM at $X_{\text{nonionic}} \geq X_{\text{nonionic,max}}$ are temperature sensitive. For these systems, increase in temperature destabilizes the formulations into two phases, an oil phase in equilibrium with a microemulsion phase. The optimum solubilization temperature (T_{U}) (i.e. the temperature at which the phase separation takes place) depends upon the type and content of the added nonionic surfactant. Addition of NaCl and cholesterol increases the thermal stability of these systems, whereas addition of urea decreases it at a comparable ω.
- The process of desolubilization of water (or aqueous NaCl) in these mixed reverse micelles stabilized in IPM has been found to be endothermic with positive entropy change. Both $\Delta\bar{H}^{\circ}$ and $\Delta\bar{S}^{\circ}$ values have been found to be higher for nonionic surfactants with larger polar head groups. The content and configuration of the polar head groups of the nonionic surfactants influence both these parameters in absence and presence of additives. Addition of NaCl increases the $\Delta\bar{H}^{\circ}$ values, whereas the contributions of cholesterol and urea upon the $\Delta\bar{H}^{\circ}$ values are not straightforward.

Acknowledgement

The authority of Indian Statistical Institute, Kolkata, is acknowledged for financial support in the form of project and Senior Research Fellowship to R.K.M.

References

[1] M.E.L. McBain, E. Hutchinson, Solubilization and Related Phenomena, Academic Press, New York, 1955.
[2] R. Nagarajan, Curr. Opin. Colloid Interf. Sci. 2 (1997) 282.
[3] M.P. Pileni (Ed.), Structure and Reactivity in Reversed Micelles, Elsevier, Amsterdam, 1989.
[4] P.L. Luisi, M. Giomini, M.P. Pileni, B.H. Robinson, Biochem. Biophys. Acta 947 (1988) 209.
[5] J.J. Silber, A. Biasutti, E. Abuin, E. Lissi, Adv. Colloid Interf. Sci. 82 (1999) 189.
[6] K. Mukherjee, S.P. Moulik, D.C. Mukherjee, Langmuir 9 (1999) 1727;
K. Mukherjee, D.C. Mukherjee, S.P. Moulik, J. Colloid Interf. Sci. 187 (1997) 327.
[7] G.B. Behara, B.K. Mishra, P.K. Behara, M. Panda, Adv. Colloid Interf. Sci. 82 (1999) 1.
[8] J. Eastoe, B.H. Robinson, D.C. Steytler, D. Thorn-Lesson, Adv. Colloid Interf. Sci. 35 (1991) 1.
[9] W.L. Hinze, Organized Assemblies in Chemical Analysis, vol. 1, JAI Press Inc., USA, 1994, p. 37.
[10] T.K. De, A.N. Maitra, Adv. Colloid Interf. Sci. 59 (1995) 95, and references therein.
[11] K. Kon-No, in: E. Matijevic (Ed.), Surface, Colloid Science, vol. 15, Plenum Press, New York, 1993, p. 125.
[12] C. Solans, H. Kunieda (Eds.), Industrial Application of Microemulsions, Marcel Dekker, New York, 1997.
[13] J. Sjoblom, R. Lindberg, S.E. Friberg, Adv. Colloid Interf. Sci. 95 (1996) 125.

[14] S.P. Moulik, B.K. Paul, Adv. Colloid Interf. Sci. 78 (1998) 99.
[15] P. Kumar, K.L. Mittal (Eds.), Handbook of Microemulsions: Science and Technology, Marcel Dekker, New York, 1999.
[16] B.K. Paul, S.P. Moulik, J. Disp. Sci. Technol. 18 (1997) 30; B.K. Paul, S.P. Moulik, Curr. Sci. 80 (2001) 990.
[17] V.T. Liveri, in: Nissim Garti (Ed.), Thermal Behavior of Dispersed Systems, Marcel Dekker, NY, 2001, p. 1.
[18] A.V. Levashov, Y.L. Khmelnitsky, N.I. Klyachko, V.Y. Chernyak, K. Martinek, J. Colloid Interf. Sci. 88 (1982) 444.
[19] P.L. Luisi, B.E. Straub (Eds.), Reverse Micelles: Biological and Technological Relevance of Amphiphilic Structures in Apolar Media, Plenum Press, New York, 1984.
[20] P.L. Luisi, L.J. Magid, CRC Crit. Rev. Biochem. 20 (1986) 409.
[21] H.F. Eicke, G.D. Parfitt (Eds.), Interfacial Phenomena in Apolar Media, Marcel Dekker, New York, 1987.
[22] E.B. Leodidis, T.A. Hatton, in: M.P. Pileni (Ed.), Structure and Reactivity in Reverse Micelles, Elsevier, Amsterdam, 1987, p. 270.
[23] A. Gupte, R. Nagarajan, A. Kilara, in: G. Charalambous (Ed.), Food Flavors: Generation, Analysis and Process Influence, Elsevier, 1995.
[24] A. Goto, Y. Ibuki, R. Goto, in: A.G. Volkov (Ed.), Interfacial Catalysis, Marcel Dekker, New York, 2002, p. 391.
[25] T. Zemb, F. Tanford, in: K. Holmberg (Ed.), Handbook of Applied Surface and Colloid Chemistry, vol. 2, Wiley, 2001, p. 159.
[26] K. Kon-No, A. Kitahara, J Colloid Interf. Sci. 41 (1972) 47.
[27] H.R. Rabie, D. Helok, M.E. Weber, J.H. Vera, J. Colloid Interf. Sci. 189 (1997) 208.
[28] K. Kon-No, A. Kitahara, J. Colloid Interf. Sci. 33 (1970) 124.
[29] K. Kon-No, A. Kitahara, J. Colloid Interf. Sci. 34 (1970) 221.
[30] K. Kon-No, A. Kitahara, J. Colloid Interf. Sci. 37 (1971) 469.
[31] R. Leung, D.O. Shah, J. Colloid Interf. Sci. 120 (1987) 320.
[32] R. Leung, D.O. Shah, J. Colloid Interf. Sci. 120 (1987) 330.
[33] M.J. Hou, D.O. Shah, Langmuir 3 (1987) 1086.
[34] M.J. Hou, D.O. Shah, J. Colloid Interf. Sci. 123 (1988) 398.
[35] V.K. Bansal, D.O. Shah, J.P. O'connell, J. Colloid Interf. Sci. 75 (1980) 462.
[36] A. Zada, J. Lang, R. Zana, J. Phys. Chem. 94 (1990) 381.
[37] T. Kawai, K. Hamada, N. Shindo, K. Kon-No, Bull. Chem. Soc. Jpn. 65 (1992) 2715.
[38] T. Kawai, K. Hamada, N. Shindo, K. Kon-No, Bull. Chem. Soc. Jpn. 66 (1993) 2802.
[39] K. Hamada, T. Ikedu, T. Kawai, K. Kon-No, J. Colloid Interf. Sci. 223 (2001) 166.
[40] J.F. Scamehorn, Phenomena in Mixed Surfactant Systems, ACS, Washington, DC, 1998; K. Ogino, M. Abe (Eds.), Mixed Surfactant Systems, Marcel Dekker, New York, 1993.
[41] M.J. Rosen, in: P.M. Holland, R.N. Rubingh (Eds.), Mixed Surfactant Systems, ACS, Washington, DC, 1992.
[42] S.J. Chen, D.F. Evans, B.W. Ninham, J. Phys. Chem. 88 (1984) 1631; D.F. Evans, D.J. Mitchell, B.W. Ninham, J. Phys. Chem. 90 (1986) 2817.
[43] M. Olla, M. Monduzzi, L. Ambrosone, Colloid Surf. A 160 (1999) 23; M. Olla, M. Monduzzi, Langmuir 16 (2000) 6141.
[44] H. Mays, J. Pochert, G. Ilgenfritz, Langmuir 11 (1995) 4347; L. Schlict, J.H. Spiligies, S. Runge, S. Lipgens, D. Boye, G. Schübel, G. Ilgenfritz, Biophys. Chem. 58 (1996) 39.
[45] K.A. Johnson, D.O. Shah, J. Colloid Interf. Sci. 107 (1985) 269; K.L. Mittal, P. Bothorel (Eds.), Surfactants in Solution, vol. 6, Plenum Press, New York, 1986.
[46] P.D.I. Huibers, D.O. Shah, Langmuir 13 (1997) 5762.
[47] G. Ludensten, S. Backlund, G. Kiwilsza, Prog. Colloid Polym. Sci. 97 (1995) 194.
[48] N. Seedher, N. Manik, J. Surf. Sci. Technol. 9 (1993) 81.
[49] D. Liu, J. Ma, H. Cheng, Z. Zhao, Colloids Surf. A 143 (1998) 59.
[50] Q. Li, T. Li, J. Wu, Colloids Surf. A 197 (2002) 101.
[51] A. Bumajdad, J. Eastoe, P. Griffiths, D.C. Steytter, R.K. Heenan, J.R. Lu, P. Timmins, Langmuir 15 (1999) 5271.
[52] C. von Corswant, O. Soderman, Langmuir 14 (1998) 3506.
[53] A. Acharya, S.K. Sanyal, S.P. Moulik, Curr. Sci. 81 (2001) 362.
[54] A. Attwood, in: J. Kreuter (Ed.), Colloid Drug Delivery System, Marcel Dekker, New York, 1994, p. 31.
[55] (a) R.K. Mitra, B.K. Paul, Colloids Surf. A 252 (2005) 243; (b) R.K. Mitra, B.K. Paul, J. Colloid Interf. Sci., in press.
[56] D.J. Mitchell, B.W. Ninham, J. Chem. Soc., Faraday Trans. II 77 (1981) 601; J.N. Isracahvili, B.W. Ninham, J. Chem. Soc., Faraday Trans. II 72 (1976) 1525.
[57] D. Liu, J. Ma, H. Cheng, Z. Zhao, Colloids Surf. A 135 (1998) 157; D. Liu, J. Ma, H. Cheng, Z. Zhao, Colloids Surf. A 148 (1999) 291.
[58] L.M.M. Nazario, T.A. Hatton, J.P.S.G. Crespo, Langmuir 12 (1996) 6326.
[59] F.O. Opawale, D.J. Burgess, J. Colloid Interf. Sci. 197 (1998) 142.
[60] H.R. Rabie, D. Helou, M.E. Weber, J.H. Vera, J. Colloid Interf. Sci. 189 (1997) 208.
[61] A. Derouiche, C. Tondre, J. Disp. Sci. Technol. 12 (1991) 517.
[62] F. Akoum, O. Parodi, J. Phys. 46 (1981) 1675.
[63] E.B. Leodidis, T.A. Hatton, Langmuir 5 (1989) 741.
[64] H. Kunieda, A. Nakano, M.A. Pes, Langmuir 11 (1995) 3302.
[65] G. Karlstorm, J. Phys. Chem. 89 (1985) 4962.
[66] R. Aveyrad, B.P. Binks, P.D.I. Fletcher, Langmuir 5 (1989) 1210; C. Solans, H. Kunieda (Eds.), Industrial Applications of Microemulsions, Marcel Dekker, 1997, Chapter 2.
[67] K. Kandori, K. Kon-No, A. Kitahara, J. Colloid Interf. Sci. 122 (1988) 78; K. Kandori, K. Kon-No, A. Kitahara, J. Disp. Sci. Technol. 9 (1988) 61.
[68] J. Kizling, P. Stenius, J. Colloid Interf. Sci. 118 (1987) 462.
[69] C. Mathew, P.K. Patanjali, A. Nabi, A. Maitra, Colloids Surf. 30 (1988) 253.
[70] H.F. Eicke, J. Colloid Interf. Sci. 68 (1979) 440; H.F. Eicke, R. Kubik, R. Hasse, I. Zschokke, in: K.L. Mittal, B. Lindman (Eds.), Surfactants in Solution, Plenum Press, New York, 1984, p. 1533.
[71] L. Mukhopadhay, P.K. Bhattacharya, S.P. Moulik, Colloids Surf. 50 (1990) 295; L. Mukhopadhay, P.K. Bhattacharya, S.P. Moulik, Ind. J. Chem. 32A (1993) 485.
[72] T.K. Jain, M. Varshney, A.N. Maitra, J. Phys. Chem. 93 (1989) 7409.
[73] A.N. Maitra, P.K. Patanjali, Colloids Surf. 27 (1987) 271.
[74] C.L.C. Amaral, O. Brino, H. Chaimovich, M.J. Politi, Langmuir 8 (1992) 2417.
[75] F.H. Farnando, M.J. Politi, Braz. J. Med. Biol. Res. 30 (1997) 179.
[76] M.B. Mathews, E.J. Hirshhron, J. Colloid Interf. Sci. 8 (1952) 86.
[77] K. Kon-No, A. Ohizumi, T. Ise, A. Kitahara, Nipon Kagaku Zasshi 91 (1970) 916; K. Kon-No, S. Kobayashi, A. Kitahara, Yakagaku 19 (1970) 489.
[78] H.F. Eicke, H. Christen, Helv. Chim. Acta 61 (1978) 2258.
[79] A.N. Maitra, J. Phys. Chem. 88 (1984) 5122.
[80] Hauser, G. Hearing, A. Pande, P.L. Luisi, J. Phys. Chem. 93 (1989) 7869.
[82] A. Goto, S. Harada, T. Fujita, Y. Miwa, H. Yoshioka, H. Kishimoto, Langmuir 9 (1993) 86.